

Predictive study of structural, electronic, magnetic and thermodynamic properties of $X\text{FeO}_3$ ($X = \text{Ag, Zr and Ru}$) multiferroic materials in cubic perovskite structure: first-principles calculations

N. MOULAY¹, M. AMERI^{1*}, Y. AZAZ¹, A. ZENATI¹, Y. AL-DOURI², I. AMERI³

¹Laboratory of Physico-Chemistry of Advanced Materials, University of Djillali Liabes, BP 89, Sidi-Bel-Abbes 22000, Algeria

²Institute of Nano Electronic Engineering, University Malaysia Perlis, 01000 Kangar, Perlis, Malaysia

³Djillali Liabes University, Faculty of Exact Sciences, Department of Physics, PO Box 089, Sidi Bel Abbes, 22000, Algeria

The full potential linear-muffin-tin-orbital method within the spin local density approximation has been used to study the structural, electronic, magnetic and thermodynamic properties of three multiferroic compounds of $X\text{FeO}_3$ type. Large values of bulk modulus for these compounds have been obtained, which demonstrates their hardness. The calculated total and partial density of states of these compounds shows a complex of strong hybridized 3d and 4d states at Fermi level. The two degenerate levels e_g and t_{2g} clearly demonstrate the origin of this complex. We have also investigated the effect of pressure, from 0 GPa to 55 GPa, on the magnetic moment per atom and the exchange of magnetic energy between the ferromagnetic and antiferromagnetic states. For more detailed knowledge, we have calculated the thermodynamic properties, and determined heat capacity, Debye temperature, bulk modulus and entropy at different temperatures and pressures for the three multiferroic compounds. This is the first predictive calculation of all these properties.

Keywords: *ab-initio; structural; electronic; magnetic; thermodynamic properties*

© Wrocław University of Technology.

1. Introduction

In recent years, the concept of multifunctional materials has attracted a great deal of attention in all areas of technological research. The multiferroic materials are a very good example for this trend, which allowed the opening of a concurrency in the field of electronic technology. This special class of materials combines several ferroic orders, like ferromagnetism, ferroelectricity, ferroelasticity, etc. [1, 2]. Interest is directed to materials that have magneto-electric coupling. Such materials are promising for several devices with novel functionalities, like magnetic-field sensors and random access memories [3, 4]. The magneto-electric effect can have several origins [5, 6]. For the BiFeO_3 , the decrease in magnetization can be compensated

by doping and fabricating thin film samples [7, 8]. Ferroelectricity is produced by the Bi-6s stereochemically active lone pair, which can only occur if the cation ionic site has broken the inversion symmetry, while the weak magnetism is mainly attributed to Fe^{3+} ions. A large ferroelectric polarization combined with a strong magneto-electric coupling has been shown experimentally by Tokunaga et al. [9]. Furthermore, the ferroelectric polarization in BiFeO_3 is induced by the peculiar magnetic structure, obtained under external magnetic field application. Several efforts of theoretical investigations have been put to better understand the behavior of these materials. It is recognized that ferroelectricity and ferromagnetism are rarely found in the same system because the conventional off-center distortion of the B ion (perovskite type oxide ABO_3) in d state, responsible for polar behavior, is usually inconsistent with the partially filled

*E-mail: lttnsameri@yahoo.fr

d orbital, which is a prerequisite for a magnetic ground state. A strategy to design structures based on symmetry principles has been proposed by Fennie [10]. The obtained results show that a polar lattice distortion induces weak ferromagnetism, and suggests that LiNbO_3 , FeTiO_3 , MnTiO_3 and NiTiO_3 materials, crystallizing under high-pressure, are good candidates for multiferroic materials classes. These results have been confirmed by the synthesis of a high-pressure form of FeTiO_3 which is ferroelectric at and below room temperature and weakly ferromagnetic below 120 K [11]. Lately, Inaguma et al. [12] have continued the same synthesis process for MnTiO_3 under high pressure and temperature. They have confirmed that this compound is also ferroelectric polar at room temperature and has weak ferromagnetism at 25 K. Many efforts have been deployed to know the nature and behavior of these multiferroic materials for their potential industrial applications.

Also, theoretical studies have been devoted to SrFeO_3 and BaFeO_3 [13]. In this paper, we present a predictive study of three multiferroic compounds of $X\text{FeO}_3$ type ($X = \text{Ag}, \text{Zr}$ and Ru). This study will be generally focused on the influence of iron on which the other items, constituting these compounds in their cubic perovskite structures, are based. Here, we will only consider the magnetic order for these compounds, using first principle density functional theory (DFT) within the local spin density approximation (LSDA).

The organization of this paper is as follows. Section 2 gives a brief overview of the methods used for calculation. Section 3 presents the results and discussion of the structural properties obtained by optimizing the energy as a function of volume. The same section is devoted to the study of electronic, magnetic and thermodynamic properties of these multiferroic compounds. Finally, the last section concludes the results.

2. Method of calculations

First principle calculations of $X\text{FeO}_3$ ($X = \text{Ag}, \text{Zr}$ and Ru) multiferroic materials have been performed using the full-potential linear muffin-tin

orbital (FP-LMTO) method [14, 15]. They have been based on density-functional theory (DFT) [16, 17] within spin local density approximation (LSDA). A crystal in this method is divided into regions inside muffin-tin spheres, where Schrödinger equation is solved numerically, and an interstitial region. In all LMTO methods, the wave functions in the interstitial region are Hankel functions. Each basis function consists of a numerical solution inside a muffin-tin sphere matched with the value and slope to a Hankel function tail at the sphere boundary. The so-called multiple-kappa basis is composed of two or three sets of s, p, d, etc. In the interstitial region, they include Fourier transforms of LMTOs. To take into account exchange and correlation effects, the local spin density approximation (LSDA), parameterized by Perdew and Wang [18], has been applied. The charge density and the potential are represented inside the muffin-tin spheres by spherical harmonics up to $l_{\text{max}} = 6$. The self-consistent calculations are considered to be converged when the total energy of the system is stable within 10^{-5} Ryd. The k integration over the Brillouin zone is managed automatically by the self-consistent calculations using the tetrahedron method [19]. The muffin-tin radius (RMT) values, number of plane waves (NPW) and the total cut-off energies used in our calculations are listed in Table 1.

3. Results and discussion

3.1. Structural properties

$X\text{FeO}_3$ multiferroic compounds crystallize in an ideal cubic structure with a space group $\text{Pm}\bar{3}\text{m}$ (#221). The structure used is shown in Fig. 1. The atomic positions and sites in the elementary cell are at (1a) X (0, 0, 0), (1b) Fe (0.5, 0.5, 0.5) and (3c) (0, 0.5, 0.5); (0.5, 0, 0.5); (0.5, 0.5, 0). To obtain different values of the structural parameters, we conducted a self consistent calculation for optimizing the energy as a function of volume (Fig. 2). In these calculations, we have used the ideal lattice parameters for the three compounds as the starting point and fitted the results with the pressure volume data to a third-order Birch

Table 1. The number of plane waves (NPW), energy cut-off (E_{cut}) and the muffin tin radius (RMT) used in our calculations for the cubic perovskite structure of $X\text{FeO}_3$ multiferroic materials.

Material	NPW	E_{cut} total(Ryd)	RMT (a.u)				
			Ag	Zr	Ru	Fe	O
AgFeO_3	9170	139.8136	3.33			1.899	1.554
ZrFeO_3	9170	139.4625		3.334		1.902	1.556
RuFeO_3	9170	145.8197			3.261	1.86	1.521

Table 2. The calculated lattice parameters (a_{eq}), bulk modulus (B_{eq}) and its pressure derivative (B'_{eq}), volume (V_{eq}), equilibrium energy (E_{eq}) for the cubic perovskite structure of $X\text{FeO}_3$ multiferroic materials.

Material	a_{eq} (Å)	V_{eq} (Å ³)	B_{eq} (GPa)	B'_{eq}	E_{eq} (Ry)
AgFeO_3	3.66	49.03	221.26	4.15	-10180.79058
ZrFeO_3	3.65	48.84	226.29	3.29	-13614.62585
RuFeO_3	3.57	45.86	312.87	3.76	-12044.46502

equation of state [20]. The calculated equilibrium lattice parameter (a_{eq}), the bulk modulus (B_{eq}) and its pressure derivative (B'_{eq}), the cell volume (V_{eq}) and the equilibrium energy (E_{eq}) in magnetic state for AgFeO_3 , ZrFeO_3 and RuFeO_3 have been obtained and are given in Table 2. The parameters values for the three compounds are in the following order: $a_{\text{eq}}(\text{AgFeO}_3) > a_{\text{eq}}(\text{ZrFeO}_3) > a_{\text{eq}}(\text{RuFeO}_3)$. Our computed values of the lattice parameters for these three compounds deviate by 0.08, 0.09 and 0.17 Å, respectively, from the 3.74 Å value found for SrFeO_3 in the earlier work [13].

We note that the use of the LSDA slightly underestimates the lattice constant. The same classification relates to the volumes values obtained for these three compounds. By contrast, a reverse situation is observed for the bulk moduli of these compounds with $B_{\text{eq}}(\text{RuFeO}_3) > B_{\text{eq}}(\text{ZrFeO}_3) > B_{\text{eq}}(\text{AgFeO}_3)$. The largest value obtained for RuFeO_3 indicates that Ru–O has a higher hardness and stiffness than both Zr–O and Ag–O ones. The latter ones have the same range of the bulk modulus value as SrFeO_3 with only a small difference [13].

3.2. Electronic and magnetic properties

We calculated total and partial densities of states of the three multiferroic compounds that are shown in Fig. 3. The plotted energy range is from -8 and -9 eV to 7 eV for AgFeO_3 , ZrFeO_3 and RuFeO_3 , respectively. The plots show a complex of strongly hybridized $4d(\text{Ag})$ - $3d(\text{Fe})$, $4d(\text{Zr})$ - $3d(\text{Fe})$ and $4d(\text{Ru})$ - $3d(\text{Fe})$ states at Fermi level. The nature of bonding for the three compounds is metallic. This behavior is also reflected in the calculated density of states for SrFeO_3 [13]. Below the Fermi level, this complex is induced by $4d(\text{Ag}, \text{Zr})$ between -1.5 and -2.5 eV for both AgFeO_3 , ZrFeO_3 compounds. The intensity of peaks for $4d(\text{Ag})$ is stronger than for $4d(\text{Zr})$. A minor contribution of $4d(\text{Ru})$ is recorded below and above Fermi level, while it is very

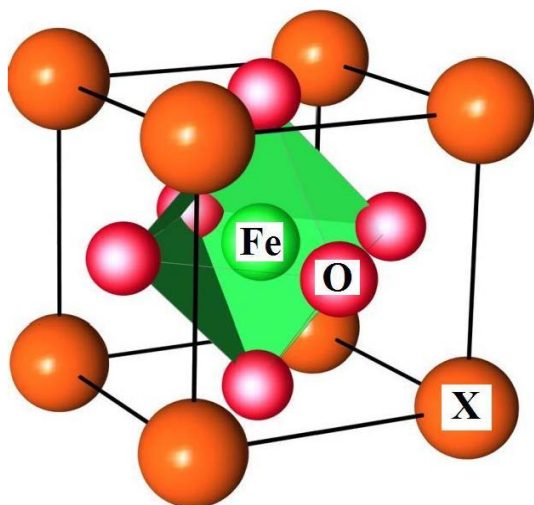


Fig. 1. An ideal cubic perovskite structure of multiferroic materials of $X\text{FeO}_3$ type.

important at Fermi level. The complex of 3d occurs above Fermi level, between energy range (E_f and 1.5 eV), just for Fe of AgFeO_3 , ZrFeO_3

multiferroic compounds. It also shows a minority contributions of 5s and 2p states for the three compounds below and above Fermi level, respectively. The plotted total and partial density of states for SrFeO_3

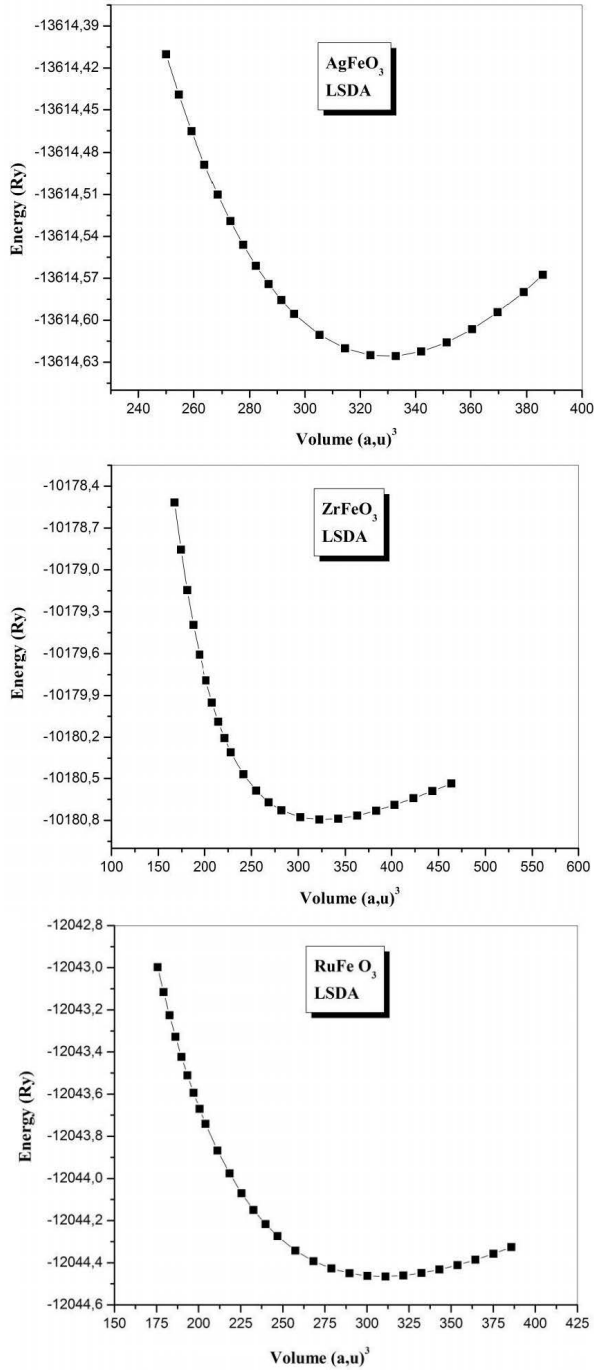


Fig. 2. Total energy versus volume for $X\text{FeO}_3$ ($X = \text{Ag}, \text{Zr}, \text{Ru}$) multiferroic materials in an idealized cubic structure.

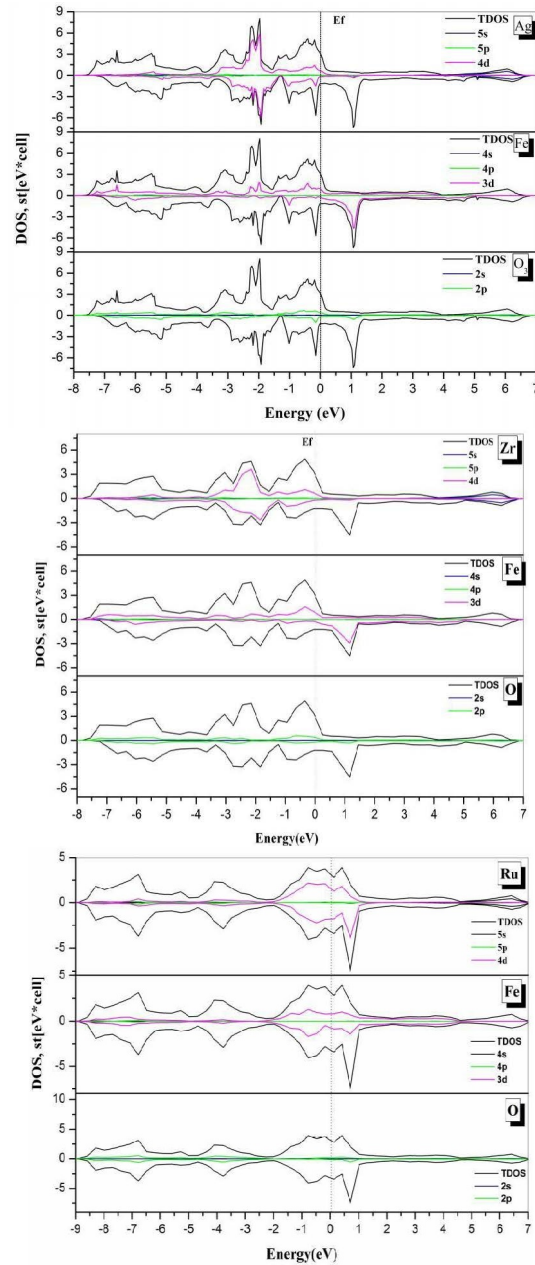


Fig. 3. The total and partial density of states of $X\text{FeO}_3$ ($X = \text{Ag}, \text{Zr}, \text{Ru}$) multiferroic materials obtained from LSDA calculation relative to Fermi level.

compound in Fig. 4 shows the similar behavior as for AgFeO_3 and ZrFeO_3 , with another peak 3d (Fe) of SrFeO_3 located at -1 eV. The corresponding peaks, due to d-orbitals of these compounds, are split by the crystal field into double-degenerated e_g and triple-degenerated t_{2g} states. The partial densities of states (P-DOS) of these two degenerate levels are given in Fig. 5. It can be seen that the contribution of 3d(Fe) comes mostly from the majority and the minority of spins of t_{2g} at the negative energies for ZrFeO_3 and RuFeO_3 , respectively, with the exception of the AgFeO_3 compound, where the peak of t_{2g} for the minority-spin of the same state is located just above the Fermi level. The exchange-splitting of the e_g and t_{2g} states for 4d(Ag) are localized at the negative energies with the highest peaks for majority and minority spin, while for the 4d(Zr–Ru), it is located above Fermi level, creating a separate peak for different energies.

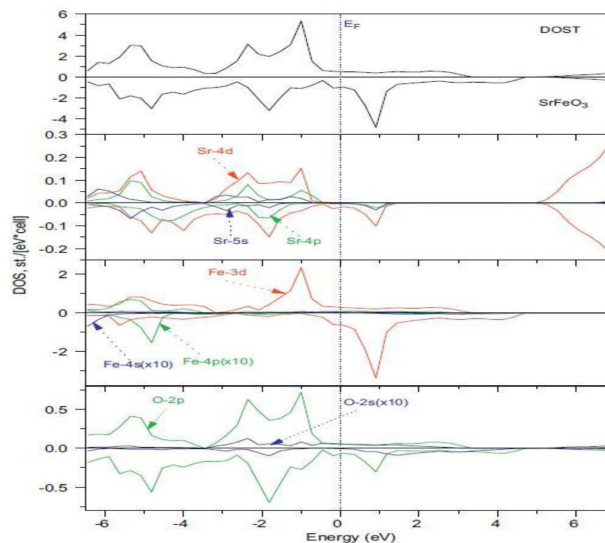


Fig. 4. The total and partial densities of states of SrFeO_3 [13].

The spin-polarized calculation gives directly the magnetic moment at $T = 0$ K. The magnetic moment is estimated using the known magnetic moments per formula unit:

$$\mu_f = 3O_{xygen} + \text{Fe} + X(\text{Ag, Zr, Ru}) \quad (1)$$

The values of magnetic moments given in Table 3 make clear that total magnetic moment per formula

μ_f for AgFeO_3 is higher than for two other multiferroic compounds. They have low values due to negative magnetic moments obtained for Zr and Fe elements.

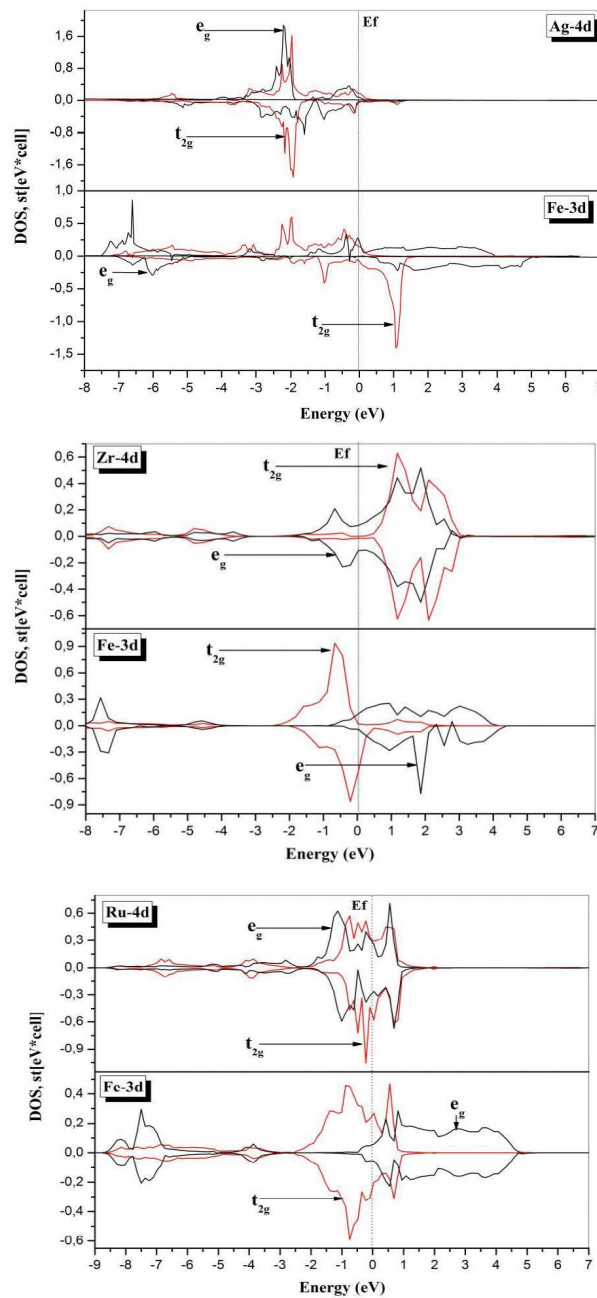


Fig. 5. The total and partial density of states of XFeO_3 ($X = \text{Ag, Zr, Ru}$) multiferroic materials obtained from LSDA calculation relative to Fermi level.

Table 3. Magnetic moments, magnetic moments per formula in elementary cell at Ag, Zr, Ru, Fe and O atomic sites and magnetization in interstitial region for $X\text{FeO}_3$ multiferroic materials.

Material	Magnetic moment (μ_B)					Magnetic moment per formula unit (μ_f)	Magnetic moment per formula unit (μ_f)
	μ_{Ag}	μ_{Zr}	μ_{Ru}	μ_{Fe}	μ_{O}	in elementary cell (μ_B)	in interstitial region (μ_B)
AgFeO_3	0.13			2.05	0.53	2.71	0.11
ZrFeO_3		-0.09		0.45	0.02	0.39	0.01
RuFeO_3			0.48	-0.03	0.06	0.51	0.005

The zirconium atom has a small induced antiparallel magnetic moment due to covalency of iron. The same behavior is observed for the iron atom with ruthenium. This confirms the ferromagnetic structure of the AgFeO_3 compound and the ferrimagnetic one in the other two multiferroic compounds. Generally, induced magnetism is caused by purely magnetic elements, which in our case is the iron, but our calculation of magnetic moment for RuFeO_3 compound listed in Table 3 gives a positive moment for pure Ru and the negative one for Fe. The origin of such situation could be attributed to the localized 4d (Ru) orbital at Fermi level.

Like in AgFeO_3 , Fe atom in the ferromagnetic compound SrFeO_3 is principally responsible for magnetic order with magnetic moment of $2.465\mu_B$. The total magnetic moment of the latter is higher than that of AgFeO_3 with a difference of $0.423\mu_B$, despite the result obtained for silver element that is higher than for strontium. Magnetism in the interstitial regions is characterized by very small values of magnetic moments for these three multiferroic compounds, like SrFeO_3 compound. The results confirm that the AgFeO_3 is a good candidate for computer technology devices, like hard disks.

We have also investigated the effect of pressure on the magnetic moments per atom for the three compounds from 0 to 55 GPa. The calculated results are shown in Fig. 6. It is easy to see close similarities between (Ag–O) and (Zr–O) of AgFeO_3 and ZrFeO_3 compounds, with the small differences between 0 and 5 GPa, where the moments decrease in the first compound and increase in the second one, and then they stabilize at higher pressures. Similar behavior is observed

for the oxygen atom in RuFeO_3 , but for ruthenium, the magnetic moment decreases with pressure. The curves of magnetic moments versus pressure for Fe atoms in the three multiferroic compounds display different behaviors. In the range from 0 to 15 GPa an increase and decrease in magnetic moments for ZrFeO_3 and RuFeO_3 compounds, respectively, is observed. On the contrary, between 25 and 35 GPa the magnetic moment in ZrFeO_3 decreases and in RuFeO_3 increases. Above 35 GPa, stability in magnetic moment values in the both compounds is achieved. Concerning the Fe atom in AgFeO_3 , we have registered a minimum of magnetic moment value of $1.16\mu_B$ between 0 and 5 GPa which then stabilized for higher pressures. As far as we know, this is the first report on the pressure dependence of magnetic moments for the three multiferroic compounds.

The different behaviors of the magnetic moment as a function of pressure have led us to a self consistent calculation to find out if transition between the ferromagnetic and antiferromagnetic states is possible. To confirm this, we have calculated the difference in the magnetic exchange energy between the ferromagnetic and antiferromagnetic states ($E_{\text{FM}} - E_{\text{AFM}}$) for the three multiferroic compounds. Generally, several magnetically ordered structures are possible for cubic perovskites of ABO_3 type, depending on the exchange interactions between B-site, oxygen and A sites [21]. The antiferromagnetic supercell configuration, assumed here, shows antiparallel orientation of the four atoms, ($X_1 \downarrow$) ($X_2 \uparrow$) as ($\text{Fe}_1 \downarrow$) ($\text{Fe}_2 \uparrow$) and the parallel one for the six oxygen atoms. The curves of the three multiferroic compounds shown in Fig. 7 confirm the stability of the ferromagnetic

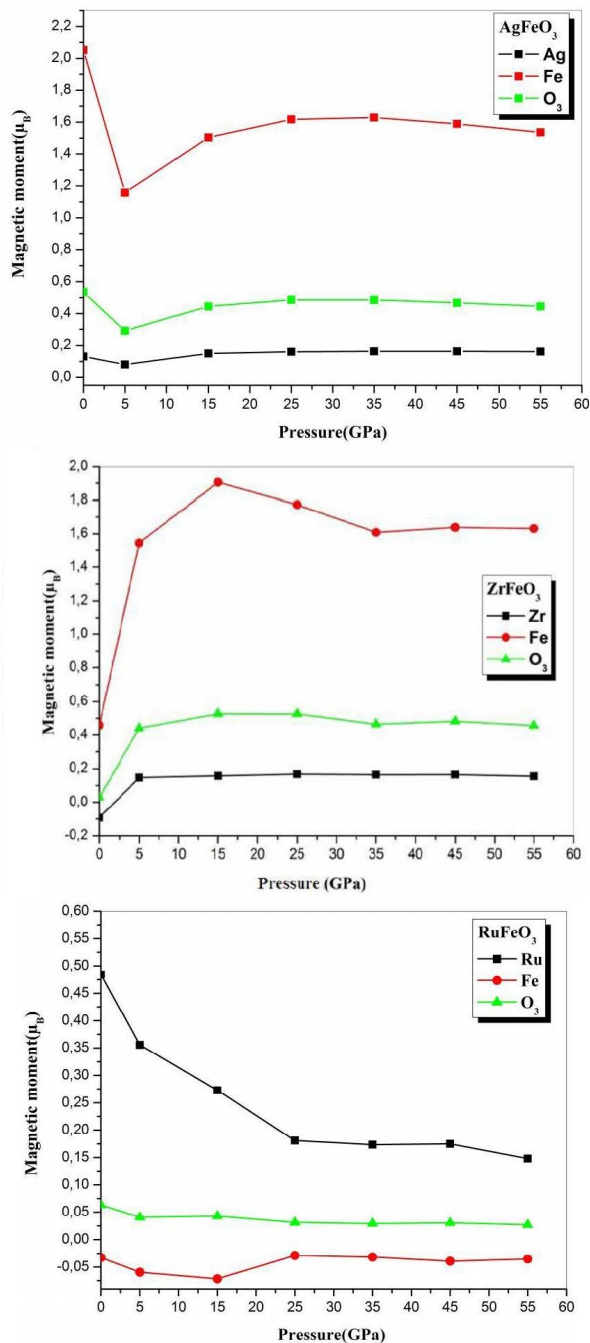


Fig. 6. Effect of pressure on magnetic moments at Ag, Zr, Ru, Fe and O atomic sites for XFeO_3 (X = Ag, Zr, Ru) multiferroic materials in LSDA calculations.

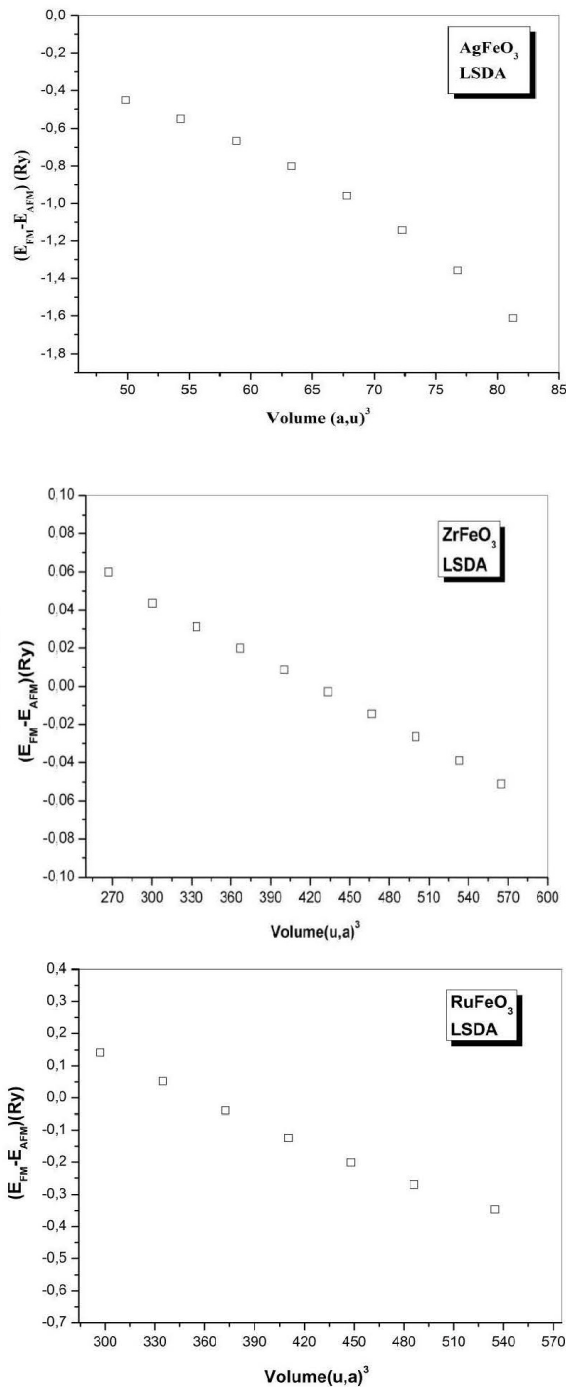


Fig. 7. Total-energy difference between ferromagnetic, E_{FM} , and antiferromagnetic, E_{AFM} , states vs. volume for XFeO_3 (X = Ag, Zr, Ru) multiferroic materials in LSDA calculations.

calculation compared to the antiferromagnetic calculation. This stability results in negative values of difference in total energies of the two phases. From

the curves, it is clear that there is no transition between ferromagnetic and antiferromagnetic states.

3.3. Thermodynamic properties

Thermodynamic properties are an important part of solid-state physics and chemistry. Moreover, investigation of these properties is of great interest to extend our knowledge on their specific behavior when submitted to the effects of high-pressure and high-temperature environments.

To investigate the thermodynamic properties of XFeO₃ (X = Ag, Zr and Ru) compound, we can apply the quasi-harmonic Debye model as implemented in the Gibbs program [23]. The quasi-harmonic Debye model allows us to obtain all thermodynamics quantities from the calculated energy-volume points, in which the non-equilibrium Gibbs function $G^*(V, P, T)$ is expressed as follows:

$$G^*(V, P, T) = E(V) + PV + A_{vib}[\theta_D(V); T] \quad (2)$$

where $E(V)$ is the total energy per unit cell, PV corresponds to the constant hydrostatic pressure condition, $\theta_D(V)$ is the Debye temperature and A_{vib} is the vibrational Helmholtz free energy. According to the quasi-harmonic Debye model of phonon density of states, one can write A_{vib} as [24]:

$$A_{vib}(\theta_D; T) = nK_B T \left[\frac{9\theta_D}{8T} + 3 \ln \left(1 - e^{-\theta_D/T} \right) - D \left(\frac{\theta_D}{T} \right) \right] \quad (3)$$

where n is the number of atoms per formula unit, K_B is Boltzmann's constant, $D(\theta_D/T)$ represents the Debye integral. For an isotropic solid, θ_D is expressed as [23, 24]:

$$\theta_D = \frac{\hbar}{K_B} \left(6\pi^2 n V^{\frac{1}{3}} \right)^{\frac{1}{3}} f(\sigma) \sqrt{\frac{B_S}{M}} \quad (4)$$

where M is the molecular mass per unit cell and B_S is the adiabatic bulk modulus measuring the compressibility of crystal, which is approximated by static compressibility as [25]:

$$B_S \cong B(V) = V \frac{d^2 E(V)}{dV^2} \quad (5)$$

$f(\sigma)$ and B_S are given. In [26, 27], the Poisson coefficient ν is taken as 0.25 [28]. Therefore, the non-equilibrium Gibbs function $G^*(V, P, T)$ as a function of (V, P, T) can be minimized with respect to

volume V :

$$\left[\frac{\partial G(V; P; T)}{\partial V} \right]_{P, T} = 0 \quad (6)$$

By solving equation 6, we get the thermal equation (EOS) $V(P, T)$. Heat capacity at a constant volume C_V and thermal expansion coefficient α are given by [29]:

$$C_V = 3nK_B \left[4D \left(\frac{\theta_D}{T} \right) - \frac{\left(\frac{3\theta_D}{T} \right)}{\varepsilon T - 1} \right] \quad (7)$$

$$\alpha = \frac{\gamma C_V}{B_T T} \quad (8)$$

where γ is the Grüneisen parameter, which is defined as:

$$\gamma = - \frac{d \ln(\theta_D(V))}{d \ln V} \quad (9)$$

Using the quasi-harmonic Debye model, it is possible to calculate the thermodynamic quantities at any critical temperature of XFeO₃ (X = Ag, Zr and Ru) compounds from the calculated E-V data at $T = 0$ and $P = 0$.

The specific heat of a material is due to the vibrational motion of the ions. However, a small part of heat is attributed to the motion of free electrons, which becomes important at high temperature, especially in transition metals with electrons in incomplete shells. The specific heat is another important thermal property, where the heat capacity of a substance is a measure of how well the substance stores heat. Whenever we supply heat to a material, it will necessarily cause an increase of temperature. This latter parameter provides an insight into its vibrational properties that are needed for many applications.

For XFeO₃ (X = Ag, Ru and Zr) materials we have investigated the thermal properties in a temperature range of 0 to 2000 K, where the quasi-harmonic model remains fully valid. We have also monitored the effect of pressure in 0 to 55 GPa range. In Fig. 8, we present the temperature-dependent behavior of the heat capacity C_V at a constant-volume. From this plot, we can distinguish two types of variations: Firstly,

it is seen that when $T < 600$ K, C_v increases very quickly with temperature for the three materials. Secondly, beyond this temperature C_v ,

increases slowly with temperature. Beyond 1250 K, C_v reaches Dulong-Petit limit and remains constant ($C_v \sim 3R$ for monoatomic solids at higher temperature). However, it can be emphasized that T_3 behavior matches the Debye model at low

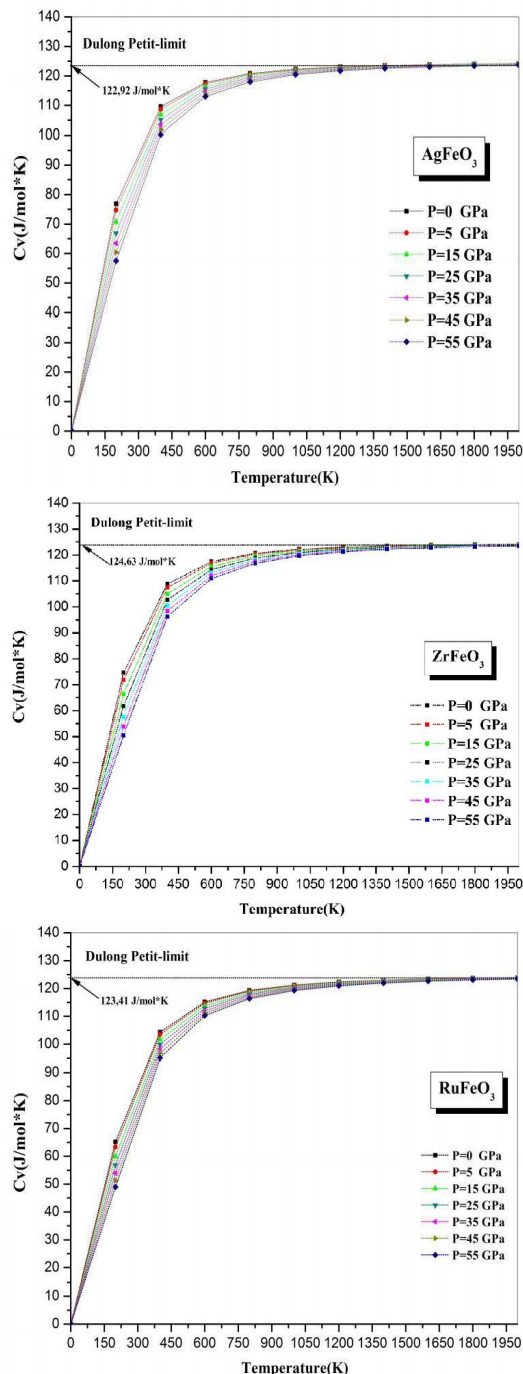


Fig. 8. The variation of heat capacity, C_v , as function of temperature at various pressures for $XFeO_3$ ($X = Ag, Ru$ and Zr).

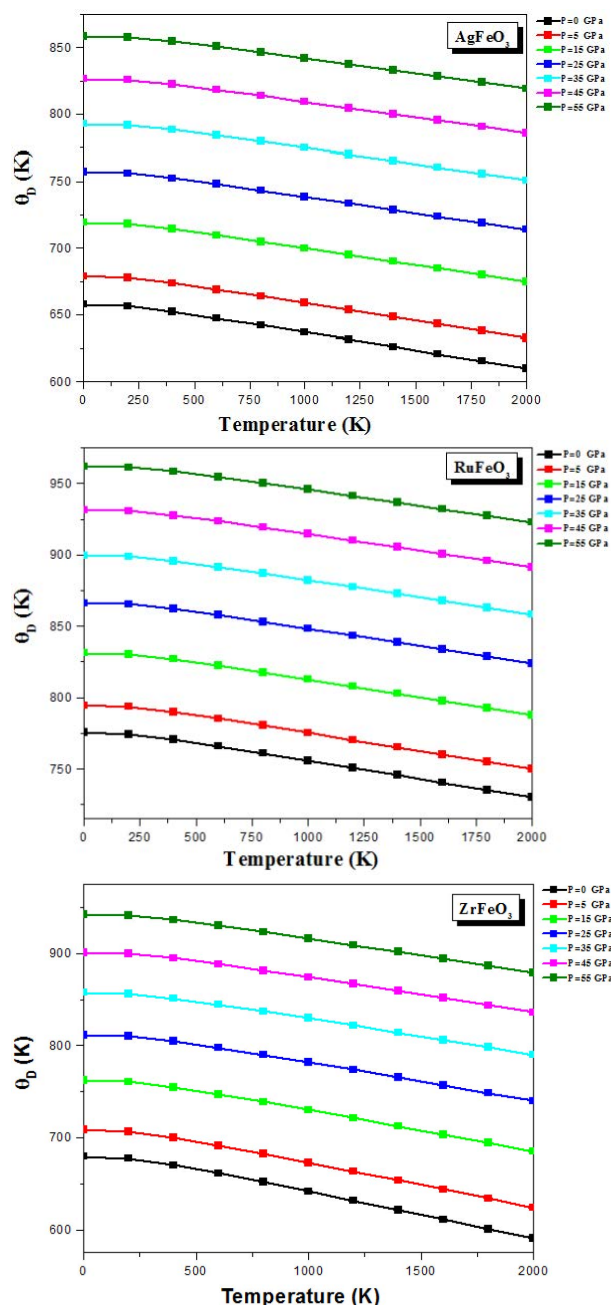


Fig. 9. The variation of Debye temperature as a function of temperature at various pressures for $XFeO_3$ ($X = Ag, Ru$ and Zr).

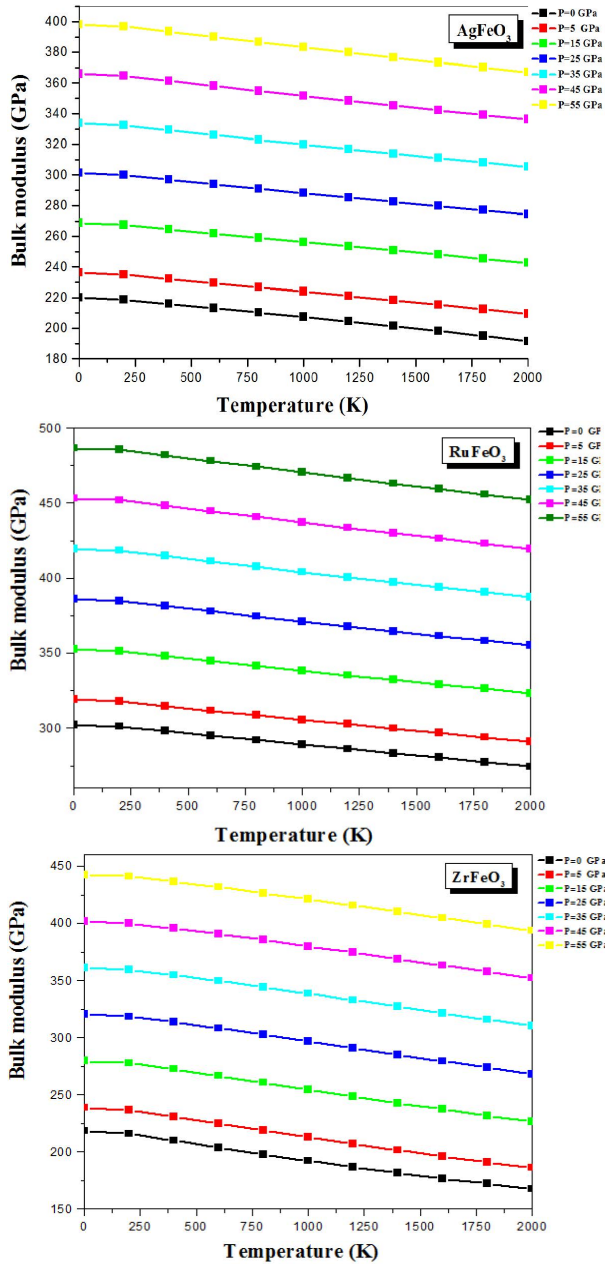


Fig. 10. The variation of the bulk modulus as a function of temperature at different pressures for $X\text{FeO}_3$ ($X = \text{Ag}, \text{Ru}$ and Zr).

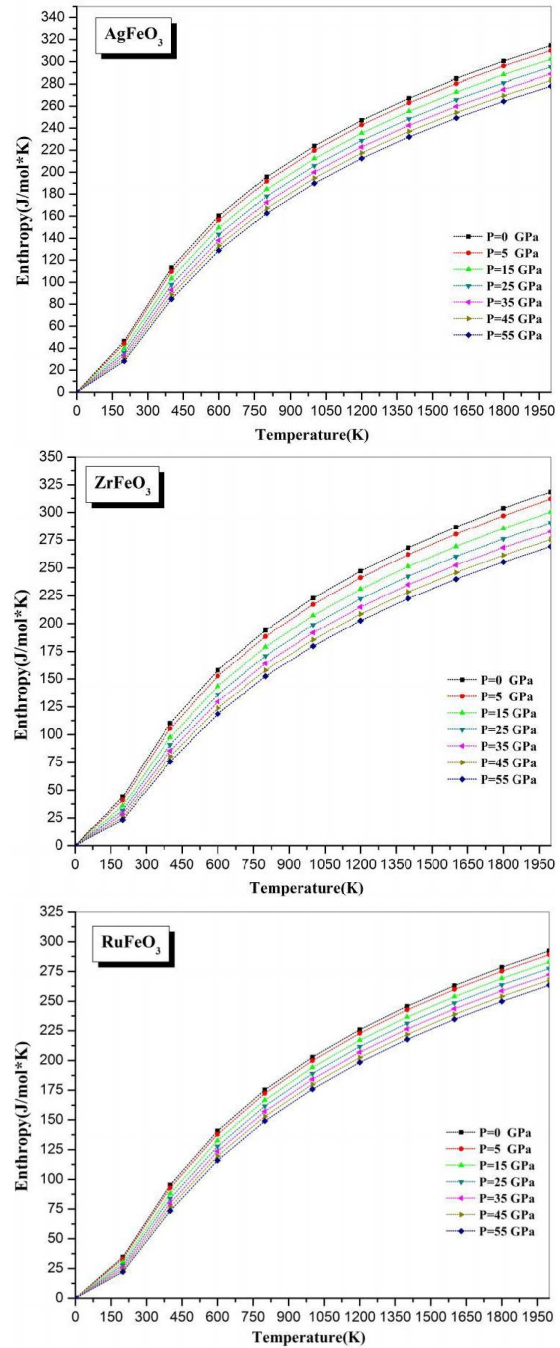


Fig. 11. The variation of the entropy as a function of temperature at different pressures for $X\text{FeO}_3$ ($X = \text{Ag}, \text{Ru}$ and Zr).

temperature. This is confirmed by the following limit values of C_v : 122.92 J/mol·K, 123.41 J/mol·K and 124.63 J/mol·K for AgFeO_3 , RuFeO_3 and ZrFeO_3 materials, respectively. It is well known that Debye temperature is an important fundamental parameter. It is closely related to many physical

properties of materials, such as elastic constant, specific heat and melting temperature. It is a temperature above which a crystal exhibits classical behavior because the phonon contribution to heat

capacity becomes more important than the quantum effect. We have plotted in Fig. 9 the evolution of the latter parameter as a function of temperature for different pressures. From Fig. 9, one can deduce the value of Debye temperature at zero pressure and zero temperature which is found to be 657.6 K, 679.6 K and 775.43 K for AgFeO₃, ZrFeO₃ and RuFeO₃, respectively.

Fig. 10 presents the variation of bulk modulus B with temperature at several pressures for the three XFeO₃ materials (X = Ag, Ru and Zr). It can be seen that the nearly constant B value is from 0 to 100 K and it decreases almost linearly with increasing temperature above T = 100 K. It indicates thermal softening of the material lattice. The compressibility increases with increasing temperature at a given pressure and decreases with pressure at a given temperature. At 300 K and zero pressure, the calculated values of bulk modulus of the materials studied here are 217.49 GPa, 213.32 GPa and 300.50 GPa for AgFeO₃, ZrFeO₃ and RuFeO₃, respectively. At zero pressure, B is lower than at higher pressures. Essentially, this implies that the multiferroic compounds are stiffened with an increase in pressure and at higher pressures the materials become stiffer. Fig. 11 represents the entropy for AgFeO₃, ZrFeO₃ and RuFeO₃ calculated as a function of the temperature at several pressures. It can be seen from that when the temperature increases, the values of the entropy (S) for AgFeO₃, ZrFeO₃ and RuFeO₃ increase gradually.

4. Conclusions

Using the FP LMTO method within the local density functional theory and LSDA approach, we have calculated the structural, electronic, magnetic and thermodynamic properties of the multiferroic compounds of XFeO₃ (X = Ag, Zr and Ru) type. The predictive values of the calculated lattice parameters for these compounds are close. These systems have large values of bulk modulus, indicating their good ductility. The calculation of their electronic structure was a challenge at the Fermi level between 4d(X) and 3d(Fe) states.

The calculated magnetic moments are negative in zirconium and iron atoms contained in ZrFeO₃ and RuFeO₃ compounds and positive in ruthenium and iron contained in RuFeO₃ and AgFeO₃ compounds, respectively. This confirms the ferrimagnetic character of ZrFeO₃ and RuFeO₃ and the ferromagnetic one of AgFeO₃ multiferroic compounds. The calculated value of magnetic moment per formula unit for AgFeO₃ is larger than the values obtained for the two other compounds but smaller than the value found in the theoretical study of SrFeO₃. The behavior of the magnetic moment per formula unit under pressure for the atoms of the three multiferroic compounds shows different variations for Ag, Zr, Fe and Ru atoms. The calculation of the magnetic exchange energy (total-energy difference between ferromagnetic state E_{FM}, and anti-ferromagnetic state, E_{AFM}) of the three multiferroic compounds does not show any transition between these two states. We also calculated the thermodynamic properties, between 0 to 55 GPa, and temperature between 0 to 2000 K. The values obtained for C_v are very close for the three multiferroic compounds. The deduced value of Debye temperature at zero pressure and zero temperature makes the difference of 117.83 and 95.83 K between RuFeO₃ and two other compounds, respectively. The calculated value of the bulk modulus of RuFeO₃ is larger than the values for the other compounds. Finally, it can be seen that when the temperature increases, the entropy values for AgFeO₃, ZrFeO₃ and RuFeO₃ increase gradually.

Acknowledgements

Y. A. would like to acknowledge University Malaysia Perlis for Grant No. 9007-00111 and TWAS-Italy for the full support of his visit to JUST-Jordan under TWAS-UNESCO Associateship.

References

- [1] RAMESH R., SPALDIN N.A., *Nat. Mater.*, 6 (2007), 21.
- [2] WANG K.F., LIU J.M., REN. Z.F., *Adv.Phys.*, 58 (2009), 321.
- [3] EERENSTEIN W., WIORA M., PRIETO J.L., SCOTT J.F., MATHUR N.D., *Nat. Mater.*, 6 (2007), 348.
- [4] SPALDIN N.A., CHEONG S.W., RAMESH R., *Phys.Today*, 63 (2010), 38.
- [5] PICOZZI S., YAMAUCHI K., SANYAL B., SERGIENKO I.A., DAGOTTO E., *Phys. Rev. Lett.*, 99 (2007), 227201.

- [6] RONDINELLI J.M., STENGEL M., SPALDIN N.A., *Nat. Nanotechnol.*, 3 (2008), 46.
- [7] BAETTIG P., SPALDIN N.A., *Appl. Phys. Lett.*, 86 (2005), 012505.
- [8] FENG H., LIU F., *Phys. Lett. A*, 372 (2008), 1904.
- [9] TOKUNAGA Y., IGUCHI S., ARIMA T., TOKURA Y., *Phys. Rev. Lett.*, 101 (2008), 097205.
- [10] FENNIE C.J., *Phys. Rev. Lett.*, 100 (2008), 167203.
- [11] VARGA T., KUMAR A., VLAHOS E., DENEV S., PARK M., HONG S., SANEHIRA T., WANG Y., FENNIE C.J., STREIFFER S.K., KE X., SCHIFFER P., GOPALAN V., MITCHELL J.F., *Phys. Rev. Lett.*, 103 (2009), 047601.
- [12] AIMI A., KATSUMATA T., MORI D., FU D., ITOH M., KYÔMEN T., HIRAKI K., TAKAHASHI T., INAGUMA Y., *Inorg. Chem.*, 50 (2011), 6392.
- [13] RACHED H., RACHED D., RABAH M., KHENATA R., RESHAK A.H., *Physica B*, 405 (2010) 3515.
- [14] SAVRASOV S.Y., *Phys. Rev. B*, 54 (1996), 16470.
- [15] SAVRASOV S., SAVRASOV D., *Phys. Rev. B*, 46 (1992), 12181.
- [16] HOHENBERG P., KOHN W., *Phys. Rev. B*, 136 (1964), 864.
- [17] KOHN W., SHAM L.J., *Phys. Rev. A*, 140 (1965), 1133.
- [18] PERDEW J.P., WANG Y., *Phys. Rev. B*, 46 (1992), 12947.
- [19] BLOCHL P., JEPSEN O., ANDERSEN O.K., *Phys. Rev. B*, 49 (1994), 16223.
- [20] BIRCH F., *J. Geophys. Res.*, 83 (1978), 1257.
- [21] WOLLAN E.O., KOEHLER W.C., *Phys. Rev.*, 100 (1955), 545.
- [22] BLANCO M.A., FRANCISCO E., LUAÑA V., *Comput. Phys. Commun.*, 158 (2004), 57.
- [23] BLANCO M.A., PENDAS A.M., FRANCISCO E., RECIO J.M., FRANCO R., *J. Mol. Struct.*, 368 (1996), 245.
- [24] FLOREZ M., RECIO J.M., FRANCISCO E., BLANCO M.A., PENDAS A.M., *Phys. Rev. B*, 66 (2002), 144112.
- [25] FAHY S., CHANG K.J., LOUIS S.G., COHEN M.L., *Phys. Rev. B*, 35 (1989), 7840.
- [26] FRANCISCO E., RECIO J.M., BLANCO M.A., PENDAS A.M., *J. Phys. Chem.*, 102 (1998), 1595.
- [27] FRANCISCO E., BLANCO M.A., SANJURJO G., *Phys. Rev. B*, 63 (2001), 094107.
- [28] POIRIER J.P., *Introduction to the Physics of the Earth's Interior*, Cambridge University Press, Oxford, 2000.
- [29] HILL R., *Proc. R. Soc. A*, 65 (1952), 349.

Received 2014-09-11

Accepted 2015-02-05